Journal of Power Sources 240 (2013) 245–251

Contents lists available at SciVerse ScienceDirect

Journal of Power Sources

journal homepage: www.elsevier.com/locate/jpowsour

Correlation of stress and structural evolution in $Li_4Ti_5O_{12}$-based electrodes for lithium ion batteries

Zungsun Choi [a], Dominik Kramer [b], Reiner Mönig [a,b,*]

[a] Institute for Applied Materials, Karlsruhe Institute of Technology, Hermann-von-Helmholtz-Platz 1, Eggenstein-Leopoldshafen 76344, Germany
[b] Helmholtz Institute Ulm for Electrochemical Energy Storage (HIU), Albert-Einstein-Allee 11, Ulm 89069, Germany

HIGHLIGHTS

- High stresses are generated upon lithiation/delithiation especially at low voltages.
- Li deficient $Li_{4-x}Ti_5O_{12}$ forms at high voltages.
- A metastable overlithiated phase forms at low voltages.
- Effects of under- and overlithiation exist even in the normal operation voltage.
- A novel *in situ* method is used for high resolution stress measurements.

ARTICLE INFO

Article history:
Received 16 January 2013
Received in revised form
14 March 2013
Accepted 27 March 2013
Available online 10 April 2013

Keywords:
Li-ion battery
$Li_4Ti_5O_{12}$
Mechanical stress
Phase transformations

ABSTRACT

$Li_4Ti_5O_{12}$ (LTO) is considered to be a "zero strain material" that shows negligible stresses upon electrochemical cycling. Here we report on the stress evolution of this material for various voltages and lithiation/delithiation rates. The features in the stress signal are correlated to the coexistence of the two phases $Li_4Ti_5O_{12}$ and $Li_7Ti_5O_{12}$ as well as to structures that form during under- and overlithiation. The formation of the under- and overlithiated structures occurs as soon as the potential deviates from its signature plateau at 1.56 V vs. Li/Li^+, where the two phases $Li_4Ti_5O_{12}$ and $Li_7Ti_5O_{12}$ coexist. In relaxation experiments time dependent phenomena in the under- and overlithiated states are investigated. Compared to other electrode materials, the stress level changes are moderate during operation at or close to the plateau voltage, but a large stress forms particularly for potentials below 1.0 V vs. Li/Li^+. This high stress accumulation which would be an adverse effect of attempts to increase the capacity by further lithiation beyond the $Li_7Ti_5O_{12}$ state is likely due to the formation of a lithium-rich phase that may compromise the reliability of this material at very low potentials.

1. Introduction

Even though LTO is commonly used and considered to be a "zero strain" material which only transitions between two very similar phases, limited knowledge exists on the detailed structural evolution of this material during battery operation including possible overcharging. In this work a novel technique consisting of high resolution stress measurements was used to investigate phases and phase transitions of LTO at different voltages and at different rates in real time during electrochemical cycling. LTO is known to be a negative electrode material that offers advantages such as superior safety, high rate capability, low cost, extended shelf life and most importantly excellent capacity retention [1,2]. The latter has been observed to be due to its exceptional low volume change of less than 0.2% as LTO transitions between $Li_4Ti_5O_{12}$ and $Li_7Ti_5O_{12}$ [3–6]. $Li_4Ti_5O_{12}$ has a cubic spinel structure with the space group $Fd\bar{3}m$ where lithium occupies tetrahedral 8a sites. Upon lithiation, additional lithium atoms occupy octahedral 16c sites while existing lithium atoms at 8a sites also move to 16c sites to minimize coulomb repulsion which eventually leads to a complete occupation of 16c sites with empty 8a sites in the $Li_7Ti_5O_{12}$ phase. Lithiation beyond $Li_7Ti_5O_{12}$ has been of interest to increase capacity and cell voltage [7–11], and has been reported to be reliable up to a few hundred cycles when cycled between voltages of 2.0 V and 0.01 V [8]. *Ab initio* calculations showed that 8a and 16c sites can be occupied simultaneously, leading up to 8.5 lithium atoms per unit cell close to 0 V [12], which corresponds to a theoretical capacity of

* Corresponding author. Institute for Applied Materials, Karlsruhe Institute of Technology, Hermann-von-Helmholtz-Platz 1, Eggenstein-Leopoldshafen 76344, Germany.
E-mail address: reiner.moenig@kit.edu (R. Mönig).

0378-7753/$ – see front matter © 2013 Elsevier B.V. All rights reserved.
http://dx.doi.org/10.1016/j.jpowsour.2013.03.185

263 mAh g^{-1}. The associated change in volume of approximately 0.4% is assumed to be reversible [12]. Although lithiation beyond $Li_7Ti_5O_{12}$ is possible it is still not clear how reliable LTO in this low potential range is. Even if there is no intended overlithiation, it may occur for non-ideal charging conditions. Besides this lack of knowledge, many details on the structural transition are not known and only limited knowledge exists on the kinetics of the individual processes. Since conventional electrochemical cycling can only show electrical degradation and does not deliver conclusive data on structural transitions, a novel approach was chosen here which consists of monitoring the mechanical stresses in the electrode during cycling. Several origins of stresses exist and among them are volumetric changes in the electrode which can be used to investigate phase transformations. In order to measure mechanical stresses and to obtain the kinetics of LTO during (de)lithiation, we have developed a laser based *in situ* substrate curvature setup. Similar experiments on electrode materials have been described in the literature [13–15], but in contrast to the study presented here they have not been performed on composite electrodes of real batteries which are porous and contain significant amounts of binder and carbon black. The low stresses that result from this porous composite structure make the measurement challenging which is further complicated by the "zero strain" nature of LTO so that a very sensitive measurement technique is needed. In this paper, we show results on the stress evolution of LTO and provide data on the kinetics of lithium insertion and extraction. Experimental evidence will be given showing that LTO no longer behaves as the "zero strain" electrode as it is lithiated beyond $Li_7Ti_5O_{12}$. The recorded data is interpreted in terms of phase transitions in which interactions between $Li_4Ti_5O_{12}$ and $Li_7Ti_5O_{12}$ phases occur and where $Li_xTi_5O_{12}$ with $x < 4$ and $x > 7$ are present. Furthermore, the mechanical response of LTO at various rates and during charge interrupts was monitored and is interpreted in terms of Li diffusion and phase transitions.

2. Experimental

2.1. Sample preparation and experimental setup

LTO composite electrodes have been fabricated with 80 wt% LTO powder (Süd-Chemie AG), 10 wt% Carbon Black (Super P), and 10 wt % Polyvinylidenedifluoride (PVDF). Battery grade copper foil was used as a current collector. The size of the LTO particles was in the micron range (Fig. 1a). The composite electrode was cut and glued to a borosilicate glass cantilever (170 μm thick, 15 mm long, 5 mm wide, Fig. 1b). The electrode was then mounted into a special home built cell with one end clamped (Fig. 2). Metallic lithium was used as a counter electrode, which was mounted and separated from the LTO electrode as shown in Fig. 2. Commercially available 1 M $LiPF_6$ in ethylene carbonate (EC) and dimethyl carbonate (DMC) solution (1:1) by Merck (LP 30) was used as the electrolyte. During filling of the electrolyte, it was made sure that the cantilever was completely immersed in the solution, since a liquid/gas phase boundary at the LTO electrode would result in additional forces due to potential-induced changes of the wetting angle and the related position of the meniscus. An optical window was placed in front of the cantilever to allow for the deflection measurement using a laser. A collimated beam from a red laser diode was aligned to be reflected from the cantilever. The setup is designed in a way that the reflected laser beam leaves the electrochemical cell normal to the glass window. The reflected beam was captured by a CMOS camera with a 1″ chip (PixeLINK PL-B782F). For this experiment, the camera was positioned at a distance of 387 mm away from the cantilever (Fig. 2). The position of the laser spot was recorded at approximately 40 Hz using a computer running a code written in LabVIEW (National Instruments). Averaging the laser intensity allowed for the determination of the spot position to within 200 nm so that changes in the radius of curvature of up to 60 km can be detected. The difference in thermal expansion of the electrode and the substrate leads to additional very strong curvature signals and needs to be suppressed during the experiment. This was achieved by placing the setup inside a thermally isolated container with active temperature control limiting the fluctuations down to less than ±5 mK. The electrochemical experiments consisted of galvanostatic charge-discharge tests of the cells with open circuit steps and were performed using a commercial battery cycler (VMP3, Bio-Logic SAS). All voltages were measured vs. a Li/Li^+ electrode.

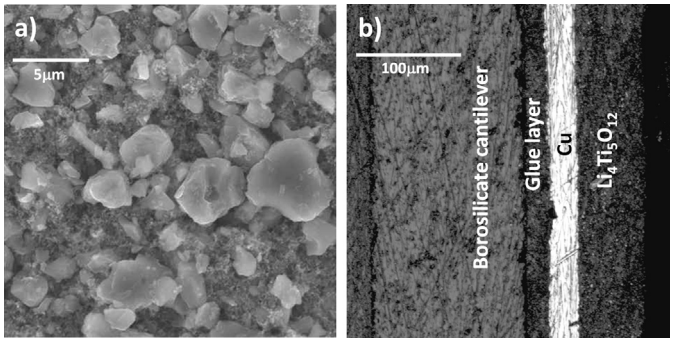

Fig. 1. a) SEM image of the composite electrode in top view and b) cross-sectional view of the electrode on the borosilicate cantilever.

2.2. Calculation of stress variations from displacement of the reflected laser beam

The bending of the layered system as shown in Fig. 1b due to mechanical stress originating from one layer is closely related to the bending of a bimetallic strip. Depending on the mechanical properties of the individual layers, different curvatures will result. For the case of a thin film on a rigid substrate which is significantly thicker than the film itself, simplifications can be made which lead to a linear relationship between stress in the thin layer and bending of the composite system given first by Stoney [16].

$$\sigma_f = \frac{E_s h_s^2}{6h_f(1-\upsilon_s)}\frac{1}{R} \tag{1}$$

In this relationship, σ is the stress, E is the Young's modulus, ν is the Poisson's ratio, h is the thickness, R is the radius of curvature. The subscripts f and s stand for film and substrate. This relation is the fundamental principle used in the substrate curvature technique and is commonly used to directly measure stresses in thin films.

A cantilever with four different layers of comparable thicknesses as shown in Fig. 1b does not fulfil the prerequisites used in the derivation of Eq. (1). Nevertheless in what follows it will be argued that a correction factor can be introduced that accounts for the deviations of this system from Eq. (1). The experiments run at constant temperature and changes are expected to only occur in the electrode layer which is the only source for the biaxial stress in the multilayer system. The electrode layer is attached to the underlying layers and upon stressing, stress responses in the other layers will result. The biaxial stress parallel to the plane of the interface is transmitted through the stack and decays towards the neutral axis of the layered system. When crossing the neutral axis, the stress changes sign to compensate the moment applied by the stress in

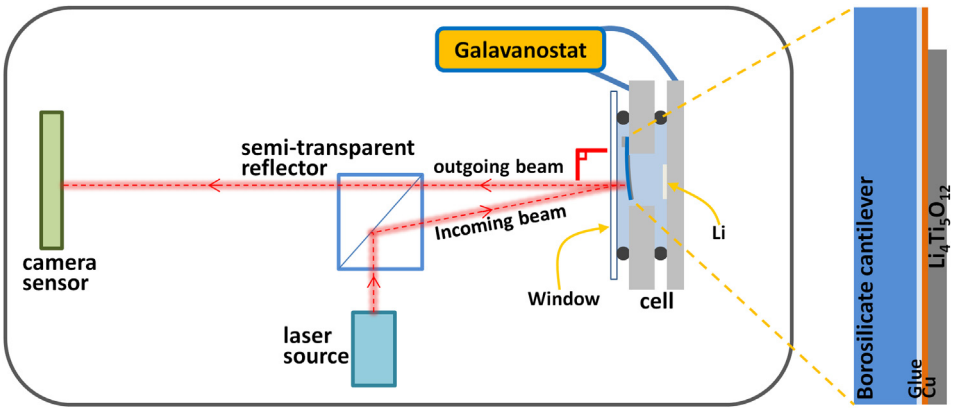

Fig. 2. Schematic image of the substrate curvature system with the cell containing an LTO composite electrode on a borosilicate cantilever and Li metal as the counter electrode. The reflected beam from the cantilever is initially aligned to be perpendicular to the window to simplify data analysis to avoid complex refraction conditions between electrolyte and air. Note that the curvature of the cantilever and the angle of the incoming beam are exaggerated.

the film. For compressive stress in the electrode film, tensile stress will result in the layers directly underneath the film and the stress and the resulting moment will be compensated by compressive stress at the back side of the cantilever. The exact location of the neutral axis depends on the mechanical properties of the layers. Since there is no simple analytical solution to this problem [17], finite element modelling of the beam was performed. Three cases were considered. In case 1 a hypothetical electrode with a thickness of 1 μm was put directly onto the glass substrate and the film was strained by a given amount. In case 2 the thickness of the electrode was increased to 62 μm (actual electrode thickness of the experiment) and the strain was also reduced by 62 times to lead to similar forces at the interface as in case 1. In case 3 the system as depicted in Fig. 1a was modelled and the strain from case 2 was applied. For the simulations the mechanical properties given in Table 1 were used. All three systems adopted a circular shape after loading. Case 1 obeys Stoney's relation. Case 2 shows a curvature that is enhanced by a factor of 1.30 (radius decreases) which is due to the additional bending moment created by the thicker electrode layer. For case 3, which is the actual cantilever used in this study, the simulated curvature is reduced by a factor of 0.587 (radius is increased) as compared to Stoney's relation. The weaker curvature can be most likely attributed to relaxations that take place in the rather soft glue layer. By introducing the correction factor $C = 0.587$ into Eq. (1), the measured curvature from the laser beam deflection can be used to estimate the average stress in the electrode layer.

A critical issue in the determination of the stress is due to the presence of the electrolyte and its optical properties. Changes in the index of refraction lead to a deflection of the laser at the transition between different media. On its way through the glass window, the laser is deflected twice, at the electrolyte/window and window/air interfaces, so that an approximately constant lateral shift occurs inside the glass. However the different indices of refraction between the electrolyte and air strongly affect the resulting deflection of the laser. In the literature concepts can be found that deal with this problem resulting from the nonlinearity of the law of refraction [18–20]. For this study, a simpler experimental approach was used where the outgoing beam leaves the cell approximately perpendicular to the glass window. This leads to small angles of deflection so that the law of refraction can be simplified to

$$\frac{n_a}{n_e} = \frac{\sin\theta_e}{\sin\theta_a} \sim \frac{\theta_e}{\theta_a} \tag{2}$$

where n is the index of refraction, θ is angle with respect to the normal of the glass window, e and a are the subscripts for electrolyte and air, respectively. The change in laser beam angle outside the electrolyte can be approximated by the product of index of refraction times the deflection angle inside the cell. This effect is known from aquariums, where the fish look bigger due to the refractive index of the water. With this linear amplification of the deflection angle at the electrolyte interface, the curvature can be estimated according to

$$\Delta\sigma_f = \frac{E_s h_s^2}{6h_f(1-\upsilon_s)}\frac{1}{n_e C}\frac{\Delta d}{lL} \tag{3}$$

where Δd is the displacement of the laser spot on the camera sensor, l is the length of the cantilever, L is the distance between cantilever and camera and C is the correction factor as determined by the finite element analysis to account for the multilayer cantilever system used in the experiments.

The measured signal is a mean value of the stresses within the composite electrode. Since PVDF and carbon black are assumed to be inactive, it is anticipated that this mean stress is correlated to volume expansion of the active material. The electrochemically inactive components and the porosity of the electrode are not expected to affect the shape of the stress signal, but may strongly influence the height of the stress amplitudes.

Table 1
Mechanical properties of the layers in the cantilever system.

	Borosilicate	Glue[a]	Copper	Electrode[b]
Young's modulus (GPa)	64	0.00007	120	2
Poisson's ratio	0.2	0.3	0.34	0.3
Thickness (μm)	137	22	26	62

[a] Mechanical properties provided by the vender.
[b] Modulus measured using nano-indentation method.

3. Results

When operated in a narrow voltage range close to the plateau voltage, as for example between 1.45 V and 1.65 V, LTO shows linear tensile and compressive stress accumulation during lithiation and delithiation respectively. Fig. 3a shows a galvanostatic cycle performed between these two voltages at a rate of C/5 where the stress signal almost adopts a triangular shape and shows only relatively small features when the current is reversed from delithiation to lithiation. A different mechanical response is found when the

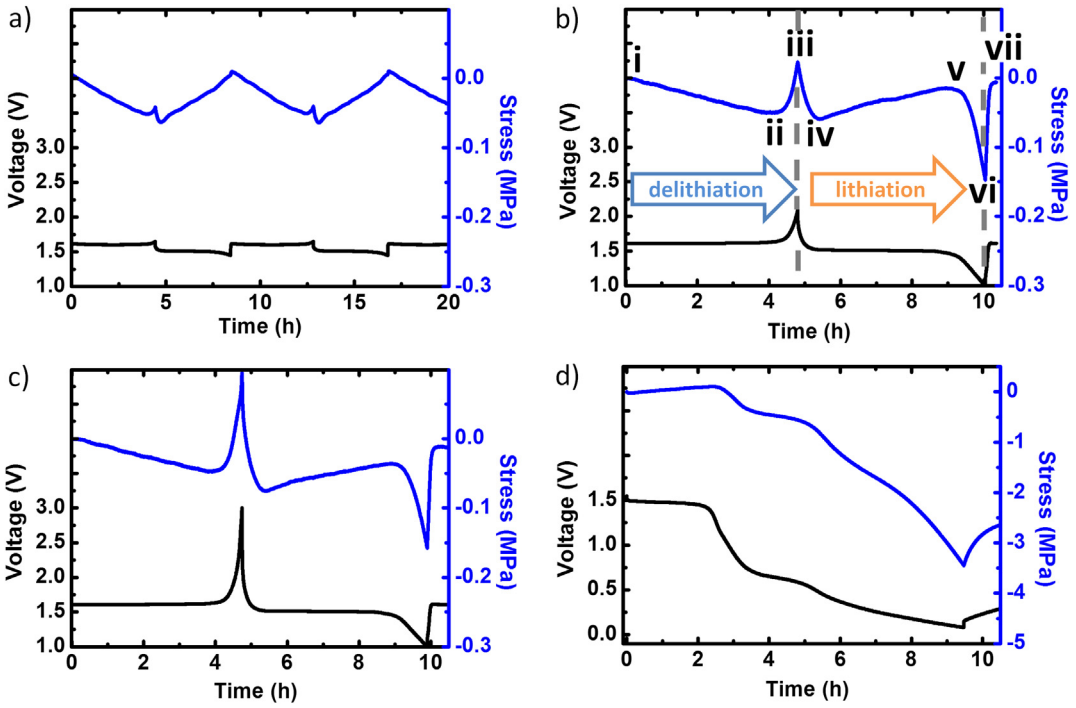

Fig. 3. Stress response during a galvanostatic cycle at a rate of C/5 with potential limits of a) 1.45 V and 1.65 V, b) 1.0 V and 2.1 V, c) 1.0 V and 3.0 V, d) a deep discharge to 80 mV. Black and blue lines correspond to potential and stress, respectively. (For interpretation of the references to colour in this figure legend, the reader is referred to the web version of this article.)

system is operated in a broader voltage range (Fig. 3b). Here the test cell was galvanostatically cycled between 1.0 V and 2.1 V at the same rate. As expected from the fact that LTO shows only small volume changes, low stress oscillations with amplitudes of roughly 200 kPa are measured. As known from Fig. 3a, a linearly increasing compressive stress of approximately 50 kPa is observed during delithiation while the potential is in the plateau region around 1.5 V (Fig. 3b from i to ii). As the voltage leaves the plateau with further delithiation, the stress moves towards tension which occurs within relatively short time and is therefore caused by a rather small change in the lithium concentration (ii to iii). At the start of lithiation at 2.1 V, the stress first moves rapidly towards compression (iii to iv), then turns again towards tension while being on the voltage plateau (iv to v). Once the voltage leaves the plateau region with further lithiation another turnaround occurs (v to vi) where the stress becomes compressive. Upon the next delithiation (vi) the stress shows a rapid tensile rise until the plateau region is reached (vii) again and the cycle restarts.

The test cell was delithiated up to 3.0 V and lithiated down to 80 mV to observe the stress responses away from the normal operating range. Fig. 3c shows the underlithiation to 3.0 V with a stress signature similar to the one in Fig. 3b and a tensile stress rise that is about twice as high as when the electrode is delithiated to 2.1 V. Compared to the underlithiation, the stress signature of the overlithiation process is more complex. It shows changes in the slope and exhibits a significant compressive stress as the potential reaches down to 80 mV (Fig. 3d). The total stress accumulation after lithiation to 80 mV is more than 70 times larger than the stress excursion found within the potential plateau at near 1.5 V.

Insights into the kinetics of the electrochemical processes can be obtained by rate variation experiments, but for LTO no significant deviation from the stress signature of Fig. 3b was found when the rate was varied between C/10 to 1C. Therefore it was attempted to obtain information on the kinetics by open circuit interruption experiments. Open circuit interrupts of 4 h were carried out after 1 h of (de)lithiation at a rate of C/5 (Fig. 4). Interrupts in the plateau regions cause only small stress excursions whereas interrupts away from the plateaus cause more significant changes. In interrupts during delithiation around the plateau region there is no significant stress relaxation but in the interrupts during lithiation there are fast but small tensile stress responses. Interrupts at the ends of (de) lithiation are depicted in detail in Fig. 5. Two distinctly different effects occur after delithiation and lithiation. In the open cell interrupt at the end of delithiation there is a relatively small stress relaxation (Fig. 5 iii to iv) where the stress becomes steady after about 2 h. If this relaxation part (iii to iv) is deleted in the signal, it

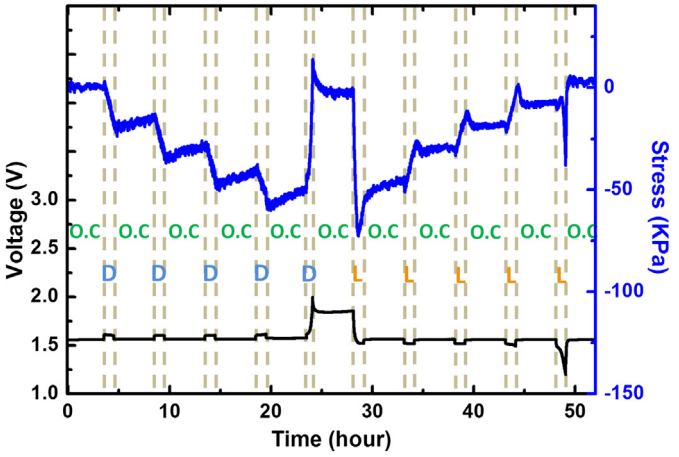

Fig. 4. Stress response during galvanostatic cycling at C/5 between 1.2 V and 2.1 V with multiple interrupts. In total 5 open circuit interrupts (for 4 h each) are performed after 1 h of delithiation or lithiation. Open circuit sections are marked as O.C., delithiation and lithiation are marked as D and L respectively. Significant stress relaxations only appear in interrupts away from the potential plateau.

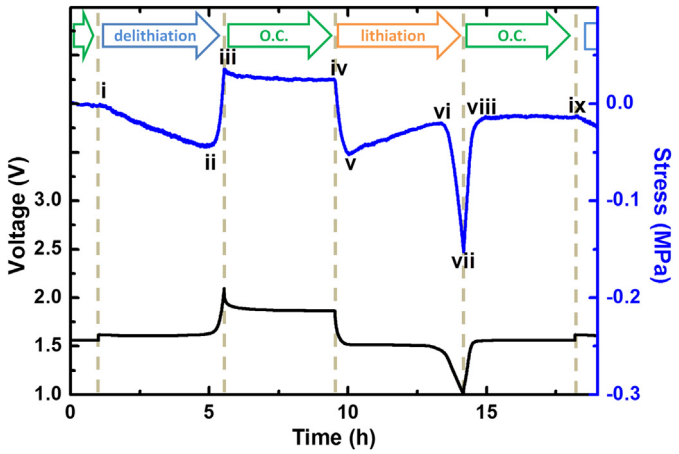

Fig. 5. Stress response during a galvanostatic cycle between 1.0 V and 2.1 V at C/5 with open circuit interrupts for 4 h (marked O.C.) at the ends of delithiation and lithiation. The stress response is noticeably larger at the end of lithiation (vii to viii) than at the end of delithiation (iii to iv).

becomes very similar to the stress signal shown in Fig. 3b (around the point iii). However, the relaxation after lithiation leads to a large and rapid tensile stress response (Fig. 5 vii to viii) where the stress saturates after less than 1 h. By comparing Fig. 5 with Fig. 3b it can be seen that a response similar to the interrupt is visible in the delithiation part of Fig. 3b (vi to vii) right after the current was reversed from lithiation to delithiation. The main difference between the two interrupts in Fig. 5 is that the interrupt after delithiation leads to only a small effect on the stress of the electrode whereas the interrupt after lithiation leads to a strong stress relaxation.

Fig. 6 compares the voltage and stress signals during interrupts after delithiation and lithiation at different rates. The relaxation of the voltage signal is observed to be very different between lithiation and delithiation. After lithiation the voltage always saturates to 1.56 V regardless of the rate (Fig. 6a). This seems to be even the case at very slow rates. In a special experiment the electrode was held at 1.0 V for 40 h and subsequently the circuit was opened again resulting in a saturation potential of 1.56 V. After delithiation there is a relaxation in the voltage signal saturating at voltages above the plateau voltage and showing larger voltage drops at higher rates (Fig. 6b). Not only the voltage, also the stress responses are different from each other. They are rather weak during delithiation compared to that of lithiation but in both cases, the magnitudes change with the rate. After lithiation an increase in rate leads to a decrease in the open circuit stress variation (Fig. 6c). However, after delithiation, an increase in rate leads to an increase in stress magnitude (Fig. 6d).

4. Discussion

4.1. Stress response during galvanostatic cycling

$Li_4Ti_5O_{12}$ has been shown to have a lattice volume that is about 0.2% larger than that of $Li_7Ti_5O_{12}$. This is likely the reason for the compressive stress buildup during delithiation and the tensile stress evolution during lithiation (Fig. 3a) as LTO makes transitions between these two phases while their volume fractions vary. When the voltage deviates from the plateau, LTO leaves the region of phase coexistence causing the stress to turn around and to rapidly

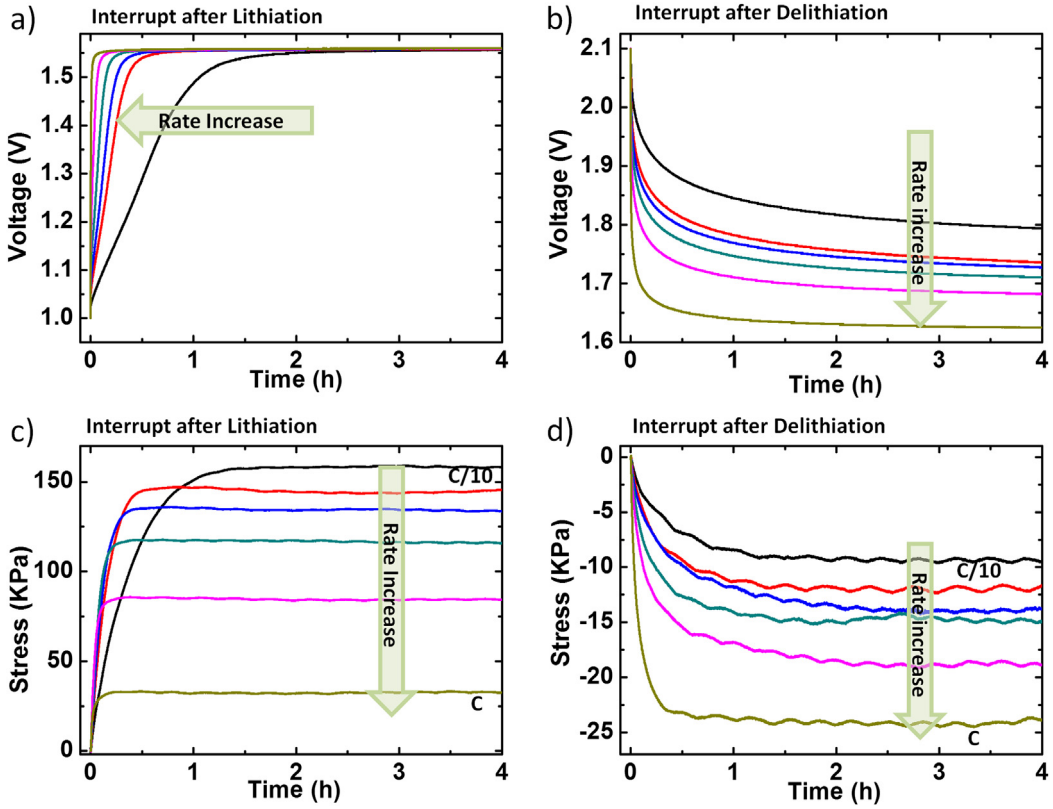

Fig. 6. Potential and stress responses during 4 h open circuit interrupts after a), c) lithiation (corresponds to Fig. 3 vii to ix) and b), d) delithiation (corresponds to iii to iv). (Dis) charge rates are C/10, C/5, C/4, C/3, C/2, and C. The start of the interrupt is chosen to be at zero stress. The stress response decreases with increasing rate after lithiation but the stress response increases with increasing rate after delithiation.

move into the opposite direction (Fig. 3b ii to iii and v to vi). The strong rise of the tensile stress shown in Fig. 3b (ii to iii) may indicate the completion of the transition from $Li_7Ti_5O_{12}$ to $Li_4Ti_5O_{12}$ and may be due to a lattice contraction caused by the underlithiation of $Li_4Ti_5O_{12}$ to Li deficient $Li_{4-x}Ti_5O_{12}$ where $4 - x$ is within the range of a stable phase of the $Li_4Ti_5O_{12}$ structure. The magnitude of the tensile stress likely correlates with the lattice volume difference between $Li_4Ti_5O_{12}$ and $Li_{4-x}Ti_5O_{12}$. At the voltage of 2.1 V this magnitude is 74 kPa, and reaches 143 kPa when the voltage is increased to 3.0 V (Fig. 3c). These stress amplitudes are higher than the stress excursions caused by the phase transition within the voltage plateau region, which are around 50 kPa. This suggests that the change in unit cell volume caused by the partial extraction of Li from the 8a sites of $Li_4Ti_5O_{12}$ can be larger than the difference in volume between $Li_4Ti_5O_{12}$ and $Li_7Ti_5O_{12}$. In X-ray diffraction experiments Rossi Albertini et al. [21] observed an abrupt decrease of the lattice parameter at the end of the delithiation and an increase of the lattice parameter at the beginning of the lithiation which is consistent with the data presented here (Fig. 3b ii to iv). However, in the same X-ray diffraction measurements the lattice parameter continuously decreases throughout lithiation which is different from the strong stress turnaround shown in Fig. 3b (v to vii). The direction of the stress turns from tensile to compressive after the end of the voltage plateau which indicates that LTO starts to go through a significant change as the lithium content increases beyond $Li_7Ti_5O_{12}$. The reason that the turnaround does not appear in the X-ray diffraction measurements could be simply due to the fact that the weight fraction of the overlithiated structure ($Li_ATi_5O_{12}$ where $A > 7$) in the particle is much smaller than the fraction of $Li_4Ti_5O_{12}$ and $Li_7Ti_5O_{12}$. If $Li_ATi_5O_{12}$ only occupies a small volume fraction and leads to a large compressive stress this would mean that $Li_ATi_5O_{12}$ has a significant structural dissimilarity compared to $Li_7Ti_5O_{12}$. This dissimilarity is supported by the pronounced compressive stress buildup of 3.5 MPa (Fig. 3d) as the cell is overlithiated. At first glance it may seem that this high stress may be due to side effects. For example solid electrolyte interface (SEI) layers are known to form on carbon surfaces below 0.8 V [22] and carbon black (Super P) starts to lithiate at around 0.4 V [23] which may also contribute to the large compressive stress accumulation. However, a stress measurement from an electrode made by the same process but without LTO (an electrode solely made from carbon black and binder) showed that the stress magnitude from carbon black alone is only about 7% that of the total stress drop measured in the electrode containing LTO. This suggests that a stress drop of 3.5 MPa results from the strong overlithiation of LTO. *Ab initio* calculations of lithiation from $Li_7Ti_5O_{12}$ to $Li_{8.5}Ti_5O_{12}$ at near 0 V show only small structural changes leading to 0.4% volume expansion [12]. This result is not consistent with the large stress magnitude present in Fig. 3d, which suggests that the structure of the overlithiated $Li_ATi_5O_{12}$ that forms during lithiation may not be the phase predicted by the *ab initio* calculations, but it is rather an intermediate phase (possibly a non-equilibrium one) probably with significant structural dissimilarity. Furthermore, in some reports discharge close to 0 V is reported to be reliable without significant degradation [7–11]. However, the massive stress evolution measured here implies that mechanical effects may play a vital role in the degradation in this voltage range.

4.2. Potential and stress response during open circuit interrupts

Stress excursions during open circuit interrupts were used to study the dynamics of the lithiation and delithiation processes. Fig. 4 shows the interrupts performed at various states of charge within one cycle. Interrupts away from the voltage plateaus lead to larger stress changes compared to that of interrupts within the plateaus. Within the plateau region two phases with very similar lattice volume coexist ($Li_4Ti_5O_{12}$ and $Li_7Ti_5O_{12}$) and redistribution of lithium between these two phases is not expected to cause strong stress signals. For voltages that are away from the plateau, more significant differences in lattice volumes ($Li_4Ti_5O_{12}$ vs. $Li_{4-x}Ti_5O_{12}$ and $Li_7Ti_5O_{12}$ vs. $Li_ATi_5O_{12}$) may exist, which may be the cause for the stronger responses in stress.

During the open circuit interrupt after delithiation to 2.1 V the stress relaxes towards compression (Fig. 5 iii to iv). The fact that the voltage simultaneously saturates to a value that is higher than the voltage plateau of 1.56 V during the open circuit interrupt indicates that the electrode equilibrates to a single underlithiated $Li_{4-x}Ti_5O_{12}$ phase. It is suspected that $Li_{4-x}Ti_5O_{12}$ is a lithium deficient structure of $Li_4Ti_5O_{12}$ where the 8a sites are only partially occupied so that the volume would depend on the concentration of lithium. Diffusion limitation will lead to gradients in the electrode and during the interrupt lithium is expected to diffuse from the regions of high concentration ($Li_4Ti_5O_{12}$) towards the lithium deficient regions ($Li_{4-x}Ti_5O_{12}$) in order to minimize energy and move towards equilibrium. This would cause a stress relaxation towards compression since in this process lithium would diffuse towards the perimeter of the particles. The accumulated tensile stress from ii to iii is rapidly released with the start of lithiation (iv to v) as $Li_{4-x}Ti_5O_{12}$ is lithiated to $Li_4Ti_5O_{12}$. However, there is only a small stress response occurring during the interrupt (iii to iv) showing that the underlithiated structure is stable without current [11].

A very different relaxation phenomenon is found in the interrupt after lithiation. Fig. 5 vii to viii shows an instant tensile rise and a subsequent saturation. The magnitude and time scale are very different from what is observed after delithiation. In this interrupt, a saturation potential of 1.56 V is achieved indicating that the system relaxes into the $Li_4Ti_5O_{12}/Li_7Ti_5O_{12}$ two-phase coexistence region. The rapid response indicates that the structure that has formed during lithiation vanishes quickly once the circuit is opened. This effect may be correlated to the formation of a structure or a phase that only forms during lithiation. Possible examples for this phase are overlithiated $Li_7Ti_5O_{12}$ or a new phase $Li_ATi_5O_{12}$ with ($A > 7$). Such a phase with high lithium content has been reported in the literature [7,8,24,25]. The coexistence of the lithium-rich $Li_ATi_5O_{12}$ with $Li_4Ti_5O_{12}/Li_7Ti_5O_{12}$ phases might be unstable; without a current, the $Li_ATi_5O_{12}$ and the $Li_4Ti_5O_{12}$ can react to form $Li_7Ti_5O_{12}$ so that a two-phase mixture of $Li_4Ti_5O_{12}$ and $Li_7Ti_5O_{12}$ is obtained again. The overlithiation experiment in Fig. 3d shows a significant stress accumulation below the voltage plateau. It is therefore plausible that $Li_ATi_5O_{12}$ has a large unit volume. In this case only small amounts of this phase would need to be formed in order to achieve the relatively high stress signal shown in Fig. 5. The presumed small amounts of this phase are consistent with the fact that this phase was not clearly discernible in X-ray diffraction measurements [21]. Since only small amounts of $Li_ATi_5O_{12}$ may exist, sufficient amounts of $Li_4Ti_5O_{12}$ may still be available in the electrode leading to the relaxation to the two-phase (plateau) state during the open circuit interrupt. Rate variations (Fig. 6a) show that the voltage signal of the relaxation after lithiation always reaches the plateau voltage independent of the lithiation rate. Furthermore, it can be seen that lower rates lead to slower voltage and stress relaxations suggesting that larger amounts of $Li_ATi_5O_{12}$ are formed and annihilated. This is in agreement with the stress levels where larger magnitudes (more of $Li_ATi_5O_{12}$) are observed at lower rates (Fig. 6c). Surprising is the fact that at the lowest rate of C/10, the voltage still returns to the two-phase region indicating that it is not possible to completely remove all of the $Li_4Ti_5O_{12}$ during overlithiation at C/10. Even when the electrode is held at 1.0 V for 40 h, the voltage returns to the plateau voltage. It therefore seems that the $Li_ATi_5O_{12}$ effectively blocks lithium insertion into the particles.

This could for example be possible if in $Li_ATi_5O_{12}$ both 8a and 16c sites are filled simultaneously so that lithium diffusion is significantly reduced. If such a phase would form at the outer perimeter of the particles it would effectively block them from further lithiation and could even preserve remaining $Li_4Ti_5O_{12}$ on their inside.

Rate variations were also used to further investigate the processes occurring in the underlithiated states (Fig. 6b, d). During relaxation after delithiation, different saturation voltages are reached depending on the rate. This shows evidence that the material is in a single phase region with different concentrations of lithium x in $Li_{4-x}Ti_5O_{12}$. At high delithiation rates diffusion limitation leads to less delithiation (higher overall concentration of lithium) and consequently during the interrupt is expected to result in larger potential drops bringing the system closer towards the two-phase region. The stress response shows larger stress drops at higher rates consistent with larger gradients inside the single phase.

5. Summary

Stress measurements based on the substrate curvature technique were used to observe the dynamic behaviour of $Li_4Ti_5O_{12}$ electrodes during galvanostatic cycling. The data was interpreted in terms of volume expansions as well as phase transformations. Stress excursions in the voltage plateau ($\sim$1.56 V) equivalent to the $Li_4Ti_5O_{12}/Li_7Ti_5O_{12}$ two-phase regime show the expected electrode contraction as the $Li_4Ti_5O_{12}$ is lithiated to the smaller $Li_7Ti_5O_{12}$ lattice. However, significant changes in the stress responses appear as soon as the potential starts to deviate from the plateau. The change in the stress response at potentials above the two-phase plateau may be explained by an underlithiation of $Li_4Ti_5O_{12}$ with partial removal of Li atoms from 8a sites while the large change in stress response at potentials below the plateau is described by the formation of $Li_ATi_5O_{12}$ with $A > 7$. Lithiation to 80 mV shows a strong compressive stress response that is more than 70 times larger than when the cell is operated in the plateau potential regime where $Li_4Ti_5O_{12}$ and $Li_7Ti_5O_{12}$ are the only phases. This large volume expansion raises the question whether this material is reliable in the low potential range. The main cause of voltage and stress relaxations during the open circuit interrupts after delithiation is suspected to be due to the equilibration of the lithium concentration in underlithiated $Li_{4-x}Ti_5O_{12}$. The voltage and stress responses during the interrupts after lithiation may be due to a transformation of the metastable mixture of $Li_ATi_5O_{12}$, $Li_7Ti_5O_{12}$, and $Li_4Ti_5O_{12}$ to the stable $Li_7Ti_5O_{12}/Li_4Ti_5O_{12}$ two-phase system. Furthermore, the difference in the (dis)charge rate dependent stress responses between relaxations after lithiation and delithiation suggests that the Li diffusion in the $Li_ATi_5O_{12}$ phase is significantly slower than Li diffusion in the $Li_4Ti_5O_{12}$ and $Li_7Ti_5O_{12}$ phases.

Acknowledgements

The authors gratefully acknowledge the help of Gabi Rizzi for finite element calculations, B.G. Yoo for measuring elastic properties of components by nano-indentation, Thomas Zevaco for determining the refractive index of the electrolyte using a refractometer and Sylvio Indris and Marco Scheuermann for helpful discussions. Z. Choi acknowledges financial support through LIB 2015.

References

[1] T. Ohzuku, A. Ueda, Solid State Ionics 69 (1994) 201.
[2] T. Ohzuku, A. Ueda, N. Yamamoto, J. Electrochem. Soc. 142 (1995) 1431.
[3] S. Scharner, W. Weppner, P. Schmid-Beurmann, J. Electrochem. Soc. 146 (1999) 857.
[4] S. Panero, P. Reale, F. Ronci, B. Scrosati, P. Perfetti, V. Rossi Albertini, Phys. Chem. Chem. Phys. 3 (2001) 845.
[5] K. Kanamura, T. Umegaki, H. Naito, Z. Takehara, T. Yao, J. Appl. Electrochem. 31 (2001) 73.
[6] M. Wagemaker, D.R. Simon, E.M. Kelder, J. Schoonman, C. Ringpfeil, U. Haake, D. Lützenkirchen-Hecht, R. Frahm, F.M. Mulder, Adv. Mater. 18 (2006) 3169.
[7] S. Huang, Z. Wen, Z. Gu, X. Zhu, Electrochim. Acta 50 (2005) 4057.
[8] H. Ge, N. Li, D. Li, C. Dai, D. Wang, Electrochem. Commun. 10 (2008) 719.
[9] H. Ge, N. Li, D. Li, C. Dai, D. Wang, J. Phys. Chem. C 113 (2009) 6324.
[10] W.J.H. Borghols, M. Wagemaker, U. Lafont, E.M. Kelder, F.M. Mulder, J. Am. Chem. Soc. 131 (2009) 17786.
[11] J. Shu, J. Solid State Electrochem. 13 (2008) 1535.
[12] Z. Zhong, C. Ouyang, S. Shi, M. Lei, ChemPhysChem 9 (2008) 2104.
[13] S.-I. Pyun, J.-Y. Go, T.-S. Jang, Electrochim. Acta 49 (2004) 4477.
[14] V.A. Sethuraman, N. Van Winkle, D.P. Abraham, A.F. Bower, P.R. Guduru, J. Power Sources 206 (2012) 334.
[15] K. Zhao, G.A. Tritsaris, M. Pharr, W.L. Wang, O. Okeke, Z. Suo, J.J. Vlassak, E. Kaxiras, Nano Lett. 12 (2012) 4397.
[16] G.G. Stoney, Proc. R. Soc. Lond. A 82 (1909) 172.
[17] P.H. Townsend, D.M. Barnett, T.A. Brunner, J. Appl. Phys. 62 (1987) 4438.
[18] G.G. Láng, M. Seo, J. Electroanal. Chem. 490 (2000) 98.
[19] T.A. Rokob, G.G. Láng, Electrochim. Acta 51 (2005) 93.
[20] X. Xiao, D. Schleh, J. Appl. Phys. 107 (2010) 013508.
[21] V. Rossi Albertini, P. Perfetti, F. Ronci, P. Reale, B. Scrosati, Appl. Phys. Lett. 79 (2001) 27.
[22] P. Verma, P. Maire, P. Novák, Electrochim. Acta 55 (2010) 6332.
[23] R. Gnanamuthu, C.W. Lee, Mater. Chem. Phys. 130 (2011) 831.
[24] H. Hain, M. Scheuermann, R. Heinzmann, L. Wünsche, H. Hahn, S. Indris, Solid State Nucl. Magn. Reson. 42 (2012) 9.
[25] S. Ganapathy, M. Wagemaker, ACS Nano 6 (2012) 8702.